

Propelling magnetic colloidal carpets on a periodic structured landscape

Carolina Rodríguez Gallo

Pietro Tierno & Helena Massana-Cid, Departament de Física de la Matèria Condensada, Universitat de Barcelona, 08034 Barcelona, Spain

Abstract—Microswimmers are artificial microscopic entities able to propel in viscous fluids and have the ability to perform tasks at the microscale. This capacity allows to impact many scientific areas such as micromanipulation, lab-on-a-chip devices or targeted drug delivery. In this study, optical video microscopy was used to examine propelled paramagnetic colloidal carpets. First, previous results were reproduced by sliding carpets on top of a flat substrate. In order to investigate more complex situations as the one occurring in natural systems, a different substrate was used. We have slid carpets on top of a periodic structured landscape, namely a two-dimensional colloidal crystal, composed of silica particles.

We observe the emergence of novel phenomena when external and time dependent magnetic fields are applied over a colloidal paramagnetic carpet driven across a periodic structured landscape. Stair-like trajectories, periodic oscillations and spontaneous reorientations of the carpet were observed. Also, the comparison of the average speed of the carpet on top of a flat substrate and on a patterned substrate is reported.

2. Nanobiotechnology: paramagnetic colloids, rotors, two-dimensional colloidal crystals.

I. INTRODUCTION

Microfluidics, the field that investigates the manipulation of microscale flow, is interesting for the fundamental understanding of fluid dynamics and physical processes in this regime^[1-5]. Many biological systems, such as blood or bacteria, are governed by the laws of fluid dynamics, making the understanding of this world crucial for the manipulation of these biosystems. For these reasons, an open field of research are microrobots or microswimmers, microscopic entities capable to generate self-propulsion and perform useful tasks at the microscale. Microswimmers are controlled by means of different approaches^[1,3,6]. Generally, they can be classified in two main groups. The first group are entities capable to generate propulsion by their own and the interaction of the surroundings, whereas the second one needs an external stimulus to obtain movement. Also there are alternative approaches that mix strategies making difficult a simple classification^[3].

In this work, we will use an external magnetic field to propel two-dimensional magnetic clusters (carpets) of self-assembled colloidal particles on top of a substrate. Previous experiments were performed on a flat surface^[7]. To investigate the effect of surface roughness and disorder, as present in real systems, here we will introduce a different type of substrate on top of which

the carpet translates. This substrate is composed of a periodic lattice of assembled non-magnetic particles. This investigation will contribute to understand the behaviour of propelling systems above heterogeneous surfaces which is more similar to real systems where the surfaces are not completely flat. Therefore, this system is also interesting in relation to tribology, as it allows investigating the sliding process between interacting crystalline surfaces with a liquid between them. Sliding velocities can be tuned by changing the parameters of the external field applied.

The work will be subdivided in four main parts. The first one will describe the theoretical concepts. In the second part there will be a description of the experimental set up, followed by the magnetic self-assembled colloidal process. Then, we will show and discuss the main results obtained with this new experimental approach and finally we will remark the conclusions and some future prospectives.

II. THEORETICAL BACKGROUND

Microscopic propelled entities submersed in a fluid deal with high viscosity. Their motion occurs at low Reynolds number, which is the ratio between the inertial forces and the viscous one. This results in fluid flows that are time reversible. All those properties generate different fluid phenomena than at the macroscale, movements that will generate net motion in the macroscale could not introduce any at low Reynolds number. This was first introduced by Purcell in 1977 with the scallop theorem^[8]. This theorem says that the dynamics of the movement of the scallop in the macroscopic world will not be useful in its micro version, since the scallop exploits the quick closing of the shell to move its body. In a viscous environment where, as said, the fluid flows are time reversible this movement will be not obtained. At low Reynolds number regime time does not matter. Slow or fast pattern of motion creates the same result. For this reason, microbiologic entities

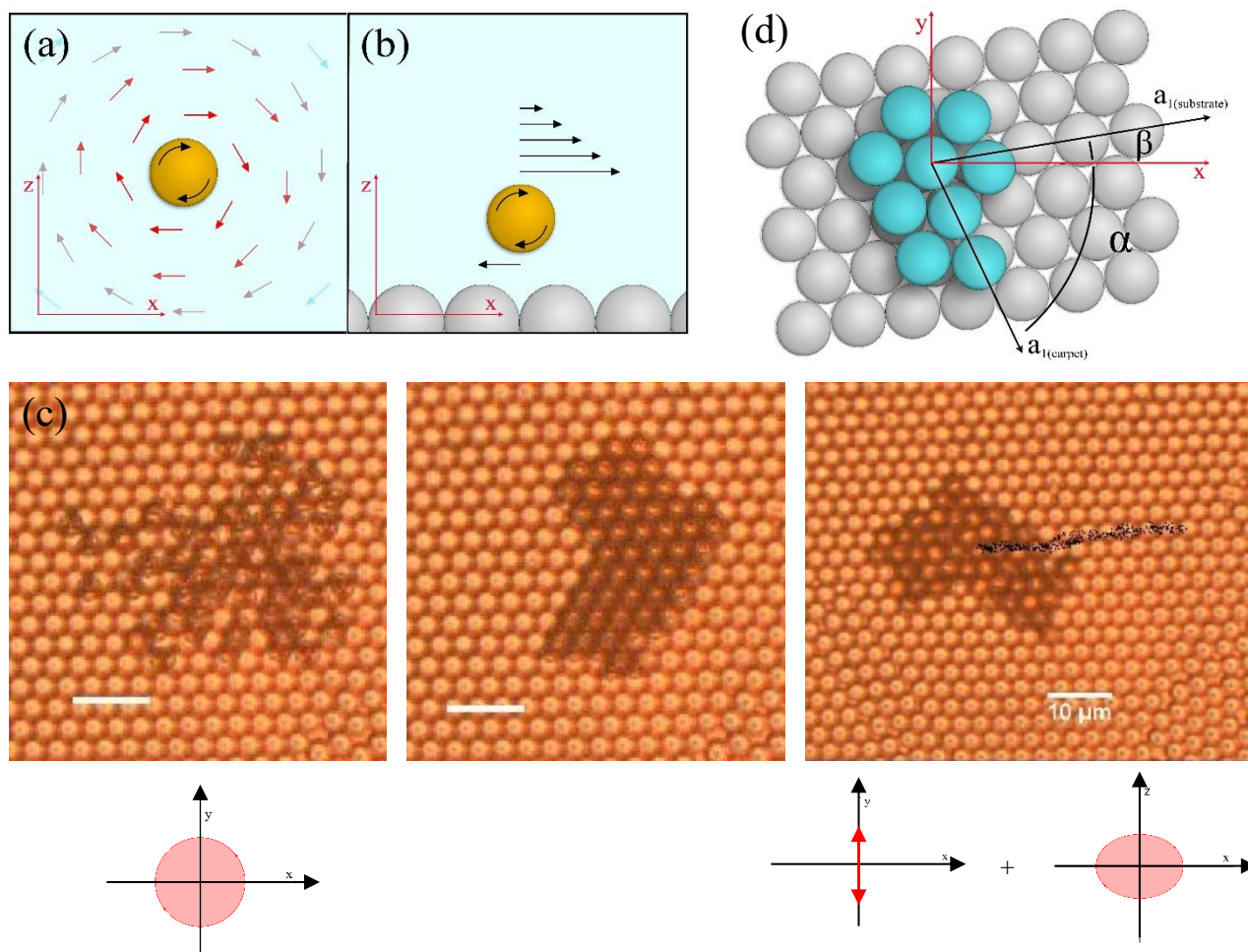


Figure 1. (a) and (b) Schematic draw of the break of the symmetry that enables the system to obtain a net movement along a desired direction. (c) Optical microscope images showing the formation and propulsion of a carpet on a patterned substrate and the magnetic field applied. (d) Sketch of the magnetic carpet (blue) above the periodic landscape (white) with the definition of angles used.

need complex techniques to swim. An example could be the flagellum of bacteria that uses a corkscrew approach to obtain translation in its body.

In this work, our microscopic entities are paramagnetic colloidal particles. The strategy used to obtain net movement is to use the hydrodynamic coupling with the walls of the container where the experiment was performed and applying a rotating magnetic field. In this way, the rotational motion of the particles is converted in a net translational one [7].

As have been predicted by Einstein [9] and after experimentally demonstrated by Perrin, a number density of colloidal particles experience sedimentation. In our case, where big particles are used, all the particles will deposit on the bottom of the container after few minutes. The proximity of the particles with the substrate, plus the rotational motion of the particles which is induced by a magnetic torque will be used in this work to obtain a net displacement at the microscale.

An external magnetic field \mathbf{H} induces a dipole moment $\mathbf{m} = V\chi\mathbf{H}$ in the particle pointing in the same direction of the field.

Here, the V is the particle volume, χ the magnetic susceptibility under a static field. By applying a rotating field elliptically polarized in the (\hat{x}, \hat{z}) plane (Fig. 1), perpendicular to the substrate plane, and because the presence of a finite relaxation time in the particles, the colloids experience an average magnetic torque of value $\mathbf{T}_m = \mu_0 \langle \mathbf{m} \times \mathbf{H} \rangle$. Where, μ_0 is the magnetic permeability of vacuum [10],[11]. This magnetic torque forces the particle to rotate around its center of mass in the (\hat{x}, \hat{z}) plane. The rotation converts in translation because of the hydrodynamical coupling with the substrate (Fig. 1(b)). Fig. 1(b) illustrates how the interaction with the bottom wall, produces a break of symmetry in the flow field generated by the rotation of the particles. Due to that symmetry breaking the particle has a net motion along the x direction. In Fig. 1(a) the bulk case is illustrated. In this case the fluid flow generated is symmetric. Hence, no net motion is obtained by the rotational one.

Until here, we have explained the case of one single rotor. By analyzing the velocities that have been obtained in this work and in previous ones from the same research group, [8] for the case of the single rotor on a flat substrate we observe low

velocities ($\sim 0.2 \mu\text{m/s}$). In microbiology applications speeds of micro propelled entities are higher. Papers of micro swimmers reviewed maximum velocities in the mm/s range ^[4]. Therefore, the strategy used in this work to obtain higher velocities is to exploit the collective behavior of the particles.

III. EXPERIMENTAL SETUP

Videos were acquired using a light microscope (Eclipse Ni, Nikon), equipped with high magnification objectives. Data were extracted from recorded videos filmed by means of a CCD camera (Balser Scout scA640-74f, Balser) mounted on the top of the microscope. The analysis of the experimental videos was performed via VirtualDub and ImageJ, two non-commercial softwares. Magnetic fields were generated by using custom-made coils arranged in a Helmholtz-like configuration. Coils were placed along the three cartesian-axis of the sample, allowing to generate magnetic fields in the 3 directions of the space. Therefore, coils allow to generate a uniform magnetic field on the sample plane and along the z direction. AC fields were obtained by connecting two coils to a wave generator (TTi-TGA1244, TTi) feeding a power amplifier (IMG STA-800, stage line or BOP 10-20 M, KEPCO). As a calibration tool a Teslometer (FM 205, Projekt Elektronik GmbH) was used. To perform experiments on a patterned structured landscape an alternative illumination set-up was used. Carpets on a periodical substrate were not easy to visualize due to the background particles. To facilitate this task, we use a mercury-fiber illumination system (C-HGFI Intensilight, Nikon) connected to an upright optical microscope via an epifluorescence tower. Blue light was obtained via fluorescent filter cube with an excitation wavelength between 450 nm and 490 nm. It allows to receive fluorescent signal from the paramagnetic colloidal particles used (Dynabeads M-270 Carboxylic Acid, Life technologies) and to better visualize the carpet from the non-fluorescent substrate. We use monodisperse paramagnetic colloidal microparticles with diameter $2.8 \mu\text{m}$, composed of a highly cross-linked polystyrene with iron-oxide nanoparticles within pores regularly distributed throughout the particles.

Samples were prepared in two different ways depending on the nature of the surface: flat or patterned. In the experiments performed on a flat surface, the colloidal suspension was introduced by capillarity in a rectangular microtube made of borosilicate glass (inner dimensions $0.1 \times 2.0 \text{ mm}$, CMC scientific) and was immediately sealed. In the other case, a drop of the colloidal suspension was placed on top of a self-assembled colloidal crystal composed by non-magnetic particles. In both cases, the particles were diluted with MilliQ water, and the concentration of the particles was varied depending on the carpet size desired. For bigger carpets a high concentration of beads was used.

To build the colloidal carpets the following approach has been used. First, a rotating magnetic field has been applied in the (\hat{x}, \hat{y}) plane (Fig. 2(c)). The applied field induces attractive dipolar interactions between the particles ^[12]. Due to this attraction, the particles form close-packed two-dimensional

clusters (carpets), as shown Fig. 2(c). After that, to obtain a net translational motion, we apply an elliptically polarized rotating magnetic field in the (\hat{x}, \hat{z}) plane. Furthermore, we will use an oscillating component in the y-axis to keep stable the structure, avoiding the separation of the particles. The overall magnetic field is given by: $\vec{H} = H_0(\cos(\omega t), \text{sen}(\omega_y t), \frac{H_z}{H_0} \text{sen}(\omega t))$. In all the experiments reported here, we have used $H_0 \equiv H_x = H_y$, $\omega = 2\pi f$ and $\omega_y = 2\pi f_y$ where $f_y = f/2$.

We clarify the nomenclature adopted in Fig. 2(d). The α angle has been defined by the area between the x-axis and the axis \hat{a}_1 of the carpet, that coincides with the larger part of the carpet, and β is the angle between the x-axis and the \hat{a}_1 axis of the 2D substrate.

IV. RESULTS

A. Preliminary study: flat surface

We start by investigating the carpet dynamics on a flat substrate, to understand the behaviour of the particles under the application of a magnetic field. We vary the different field parameters, such as the plane in which the field is rotating and the direction, clockwise or counter-clockwise. By changing the sign of the field in the z-axis the carpet inverts the motion direction. By changing the plane of the rotating magnetic field, movement along the $\pm y$ -axis has been obtained. Therefore,

TABLE I
MAGNETIC FIELD CONFIGURATION OF THE MOVEMENTS

Applied magnetic field	movement
$\vec{H} = H_0(\cos(\omega t), \text{sen}(\omega_y t), \frac{H_z}{H_0} \text{sen}(\omega t))$	\rightarrow
$\vec{H} = H_0(\cos(\omega t), \text{sen}(\omega_y t), -\frac{H_z}{H_0} \text{sen}(\omega t))$	\leftarrow
$\vec{H} = H_0(\text{sen}(\omega_y t), \cos(\omega t), \frac{H_z}{H_0} \text{sen}(\omega t))$	\uparrow
$\vec{H} = H_0(\text{sen}(\omega_y t), \cos(\omega t), -\frac{H_z}{H_0} \text{sen}(\omega t))$	\downarrow

carpets are freely to move along the two-dimensional plane on command. Parameters needed to achieve the desired direction of propulsion are shown in table 1.

Moreover, we vary in the experiments also the number of particles forming the carpet and investigate how the mean speed depend on this parameter. These results are shown in Fig. 2. In Fig. 2 a growth of the average velocity by increasing the number of particles is observed, furthermore a plateau seems to appear for carpets composed by tens of particles. Meaning that the cooperative effect of the magnetic rotors reaches its maximum efficiency. Previous experiments reported velocities up to $6 \mu\text{m/s}$ when increasing the number of particles further, and the strength of field applied ^[7]. Nevertheless, the velocity reaches a plateau around $N \sim 130$ particles. Meaning that at a certain point, particles are too far away to feel the contribution of the

generated flow field from the other particles belonging to the carpet.

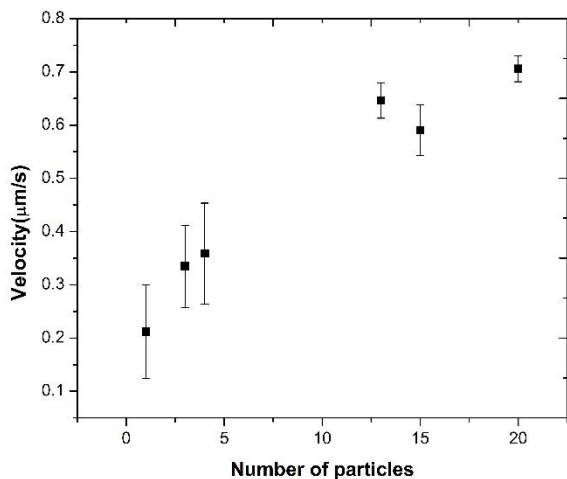


Figure 2. Average translational speed versus N , number of particles composing the colloidal carpet. The magnetic field applied was : $\vec{H} = H_0(\cos \omega_x t, \sin \omega_y t, \frac{H_z}{H_0} \sin \omega_x t)$, where $H_0 = 1.8 \text{ mT}$, $H_z = 0.9 \text{ mT}$, $f_x = 40 \text{ Hz}$ and $f_y = 20 \text{ Hz}$. Each point of the figure corresponds to a statistical average of 5 different measurements of the carpets having approximately a spherical shape and the error bar corresponds to the standard deviation.

B. Self-assembles 2D colloidal silica crystals: growth technique

To obtain a periodic landscape we self-assemble a two-dimensional (2D) colloidal crystal composed of silica particles. It was important to obtain domains, without defects and as big as possible to be able to perform experiments not only with small carpets but also with big ones. We try different growth techniques in order to find the best method to reduce the number of defects as disclinations and dislocations [13].

The building blocks of these 2D crystals were micro particles based on silicon dioxide and having $3 \mu\text{m}$ diameter. We assemble them using a water solution containing 10 mM of NaCl which screens the electrostatic interactions between the particles and favours attractive Van der Waals interactions to dominate. Even though different reviewed techniques were tested, the best results have been obtained by means of spin-coating. The parameters that were tuned to optimize the obtained results were: the revolutions per minute, spin time application and the concentration of the colloidal solution. The best performance of these technique was obtained with 500 rpm during 1 min with a solution of 95 wt%. Without defects crystal domains of around $\sim 400 \mu\text{m}^2$ were obtained. Other techniques allowed to build crystals domains of around $\sim 200 \mu\text{m}^2$. Other techniques employed to obtain two-dimensional crystals were: to build the crystals on a 9° -tilt substrate; to alter the evaporation rate by introducing ethanol in the particle solution and changing the particles concentration. Although micron-sized crystal domains were obtained, results were not satisfactory due to the poor reproducibility and the small area without defects obtained. With those techniques we obtained mostly triangular

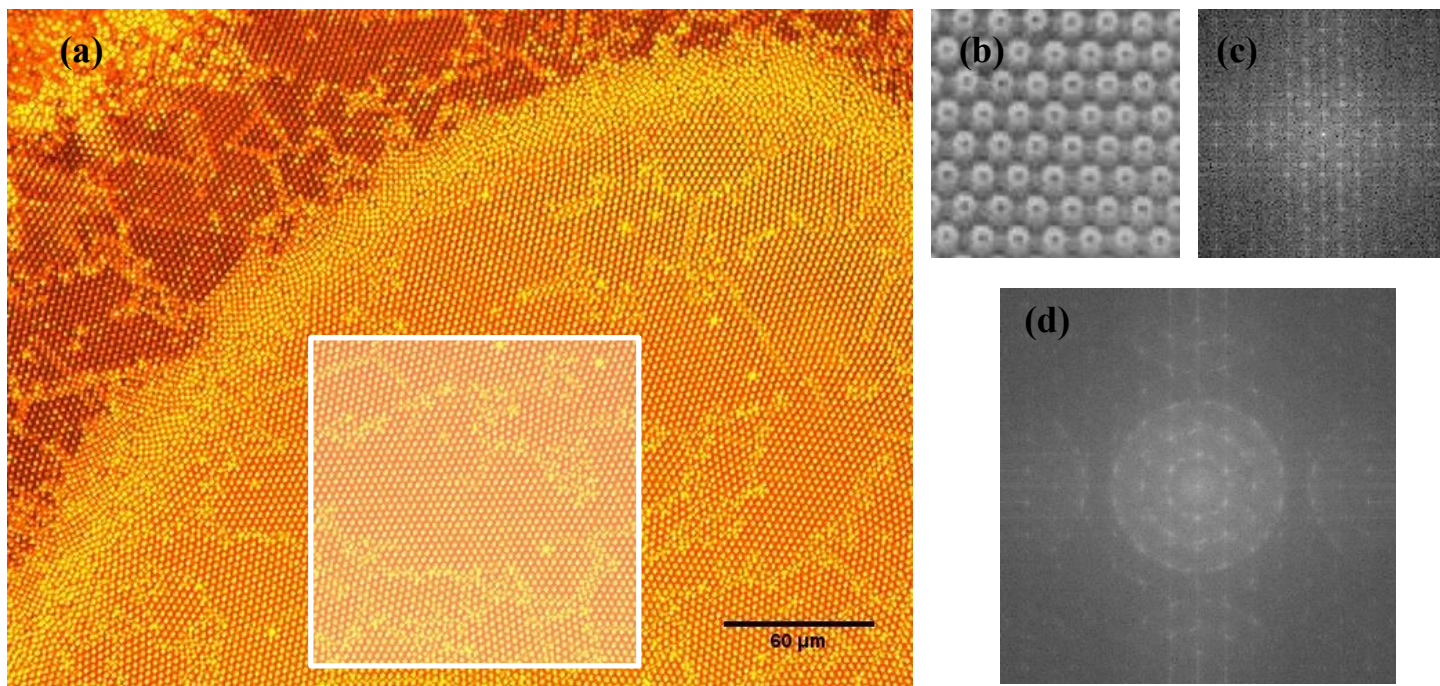


Figure 3. (a) Microscope image of two-dimensional colloidal crystals of silica particles obtained by means of the spin-coating technique. In the upper left part of the image also 3D crystals are observed. (b) Single crystal domain. (c) Fast Fourier Transform (FFT) of the single crystal domain. (d) Corresponding FFT of white area.

lattice crystal arrangement of the silica microspheres (Fig. 3). However, also two-dimensional cubic arrangement and three-dimensional hexagonal crystals were observed, as shown Fig. 3(a). Also, a high density of defects was observed mainly in the intersection of different domains. Line defects or vacancies were also seen. Fig. 3(c) shows the Fast Fourier transform (FFT) of a microscope image of a single crystal domain. Spots corresponding to the reciprocal lattice of a triangular lattice are observed. Fig. 4(d) shows in addition to single spots blurry rings, introduced by the polycrystalline character of the substrate. The periodic structured substrate has a lattice parameter of $(3.11 \pm 0.02) \mu\text{m}$.

C. Carpet trajectories on a periodic structured landscape

After preliminary studies on a flat substrate, we investigate the propulsion of the carpet above the colloidal crystal.

The position versus time exhibits a fluctuating trajectory (Fig. 4 (a,b)) with changes in the instantaneous velocity. That might be because particles are momentarily trapped in the pattern cavities. The stair-like trajectory behaviour is highly dependent on carpet-substrate orientation. Generally, if crystallographic axes of carpet and surface are aligned this behaviour is more noticeable.

By increasing the carpet size new phenomena appears. In addition to stair-like trajectories an oscillatory component is observed. Even though this phenomenon is still not completely understood experiments have been performed in order to figure out the possible causes and dependencies of the oscillations. For that purpose, different experiments were carried out by changing the number of particles, the carpet-surface orientation and the strength of the magnetic field. Experimental data is shown in Fig. 4(b). A periodic oscillation of the centre of mass position of the carpet is observed. These oscillations do not coincide with the particles position of the substrate, as it occurs with the stair-like trajectories. Oscillations have a higher periodicity and frequency.

In other experiments, all the parameters were kept constant ($N = 88$, $\beta = 0^\circ$, $f_x = 40$ Hz) and trajectories were recorded by changing the strength of the field from 0.7 mT to 3 mT. Oscillations with a frequency near ~ 1 Hz were observed in all the trajectories. Changes in the amplitude of the field do not introduce noticeable changes below 2 mT values. The frequency of oscillations remains constant and the variation of the amplitude seems to not alter the system. This oscillation is no longer observed for amplitudes higher than 2 mT. The speed of the carpet increases and the interaction that generates this oscillatory motion is evaded.

We also report the continuous change in time of the angle α . Spontaneous reorientations of carpets were observed during experimental procedures (Fig. 4(c)). This change on the angle α during the magnetic propulsion was not observed for larger carpets on flat surfaces [7]. Therefore, this reorientation might be caused by the periodic structure in the bottom of the carpet. No conclusive results have been obtained in this work about this spontaneous reorientation. Reorientation might be caused by the meeting of the carpet with an easy axis of the substrate that will generate a non-spontaneous reorientation, due to poor rigidity of the carpet. That will force the carpet to follow this crystallographic direction.

As Fig. 4(c) shows, fluctuations of the angle are high since reorientations up to 70° are obtained. This reorientation was also observed under different magnetic field conditions and with different carpets shape and size.

D. Average speed dependence on the magnetic field amplitude

We have also performed some experiments to characterize the average carpet velocity when the amplitude of the field changes. On a flat surface experiments, it has been shown that the amplitude dependence of the average velocity is quadratic [7], [14]. Also a theoretical model has been fitted to the experimental data. Here, we report results on a flat surface and on a periodic structured landscape with the objective to compare both dependencies. We have performed both

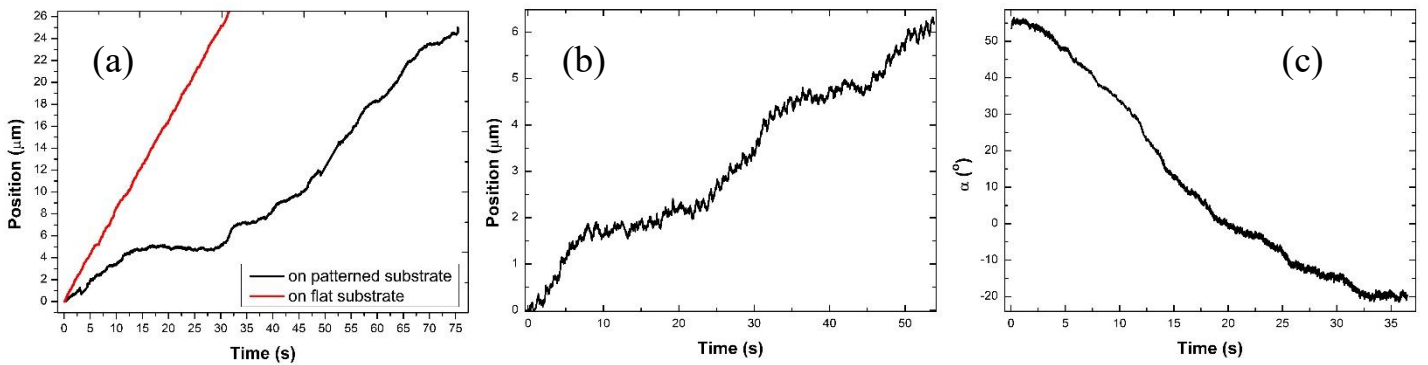


Figure 4. (a) Trajectory of a $N = 15$ carpet. Red points correspond with the trajectory of the center of mass of the carpet on a flat substrate whereas points line correspond with the trajectory on patterned substrate. The carpet parameters are $N = 15$, and $\alpha = 41^\circ$ and $\beta = 24^\circ$. The field applied was $\vec{H} = H_0(\cos \omega_x t, \sin \omega_y t, \frac{H_z}{H_0} \sin \omega_x t)$, where $H_0 = 1.85$ mT, $H_z = 0.9$ mT, $f_x = 40$ Hz and $f_y = 20$ Hz. (b) Oscillations observed in the trajectory of the carpet ($N = 34$) when the number of rotors increases. In here, $\beta = 0^\circ$, the field applied has values of $H_0 = 0.85$ mT, $H_z = 0.41$ mT, $f_x = 40$ Hz and $f_y = 20$ Hz. (c) Carpet reorientation over time. $N = 53$.

experiments with the same carpet size $N = 34$ and by also keeping the β angle constant and equal to 0° . That means the x-direction of the field corresponds with one of the three crystallographic axes of the substrate. As shown in Fig. 5, on a periodic structured substrate the carpet displays lower average speed. This behaviour was expected since the interaction with the substrate causes temporal trapping of the particles composing the carpet within the holes of the pattern. This results in an overall reduction of the propulsion efficiency. By fitting the experimental data with the model in Ref. [14] we can extract the magnetization relaxation time of the particles that normally on flat surface experiments is around $\tau_s = 10^{-4}s$. We will use τ_s as an adjustable parameter to examine if the data acquired keep to the theoretical model. By fitting the on flat substrate data, we have obtained $\tau_s = 0.5 \times 10^{-4}s$. Magnetic relaxation time is in accordance with previous experiments [14]. On periodic structured landscape data have surprisingly the same tendency as the on flat surface one. This result is unexpected since, analysing individual cases, differences has been observed. This similarity might be caused by the small carpet size employed, that is not enough to generate observable interactions when a statistical data approach is used. Alternatively, the experimental set up of this experiment does not highlight the differences among both approaches. By changing the used parameters and a large carpet area, we expect to observe noticeable differences.

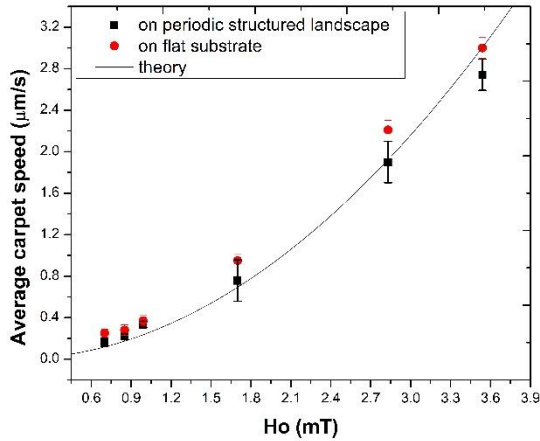


Figure 5. Average speed of the carpet vs. amplitude of the magnetic field. Red dots correspond to data of carpet traveling above a flat surface, while black dots are data collected on a periodic landscape. The number of particles of the carpet is $N = 34$ in both experiments and $\beta = 0^\circ$. In the fitting we have used: $h = 2.6 \mu\text{m}$, $l = 3.2 \mu\text{m}$, $\chi = 0.4$ and $H_0/H_z = 1/0.481$.

V. CONCLUSIONS AND FURTHER PROSPECTS

We have observed different behaviors of the propelling carpets when the flat surface is substituted by a periodic substrate. The main results were the observation of a stair-like trajectory, the presence of periodic oscillations in the carpet trajectory and the orientational motion in large carpets. Stair-like trajectory

reflect the fact that the carpet is sensible to corrugations of the substrate. This behavior was observed for small and large carpets and under different field conditions.

Moreover, when the carpet area increases, a stronger carpet-substrate interaction is observed that generates periodic oscillations in the carpet trajectory. Also, spontaneous reorientations of large carpets were observed, up to 70° .

Finally, a comparison between both cases was performed by analyzing the average speed of the carpet upon variation of the field strength. Similar tendencies have been observed, and this similarity might be due to the small areas of the carpet used and the lack of enough statistical data analysis.

These results encourage to perform further experiments. The first limitation that we have found is the small area of uniform domains of the underlying colloidal crystal, which restricts the dimensions of the paramagnetic carpet. Using electron beam lithography to obtain higher crystal domains might be a possible way to build larger two-dimensional periodic crystals. Moreover, the diameter of the particles that belong to the substrate can be tuned to observe in which way it affects the carpet trajectory. In other works [15] orientational and directional locking effects with a fast reorientation of stiff clusters were observed with different lattice parameter. Previous studies [15] were performed with rigid structures. In our case carpets are not rigid, particles suffer repulsive electrostatic interactions among them, that could induce stresses and deformations during propulsion, which could also be studied further.

To conclude, we highlight the potential of this system to give rise to a surface-surface interaction phenomenon that will have potential applications in tribology, as well as could provide fundamental knowledge of surface-surface interactions.

APPENDIX

THEORETICAL MODEL

The theoretical model used to fit the experimental data was the one in Ref [14]. In here, we report the equations and parameters used.

In a dynamic field $\mathbf{H}(t)$ rotating in the (\hat{x}, \hat{z}) plane the paramagnetic colloid is exposed to a magnetic torque with value:

$$T_c = \frac{H_0 H_z V \chi \tau_r \omega}{\mu_0 (1 + \tau_r^2 \omega^2)} \hat{x}$$

In the regime of $\omega \tau_r \sim 1$, where ω is the angular frequency and τ_r the magnetization relaxation time ($\tau_r \sim 10^{-4}s$ in our paramagnetic colloids), the particle will rotate with an angular velocity smaller than the applied one.

The mean speed of a carpet in $(0,0)$, by considering each paramagnetic colloid as a rotor is:

$$v \cong T_c \left(\frac{a^2}{32\pi\eta h^4} + \frac{1}{4\eta l^2} \right) e_y$$

a is the particle radius, η the viscosity of the medium, h the distance of the carpet from the surface due to double layer effect and l the triangular lattice parameter.

In order to fit experimental data with the theoretical model we have used along all the experiments a constant H_0/H_z value.

ACKNOWLEDGMENT

I would like to acknowledge my tutor Pietro Tierno for his always open door and Helena Massana Cid for her support in the laboratory and the continuous encouragement during this work. I would also like to thank my friends and family for their patience and help during this study.

REFERENCES

- [1] Dreyfus, R., Baudry, J., Roper, M. L., Fermigier, M., Stone, H. A., & Bibette, J. (2005). Microscopic artificial swimmers. *Nature*, *437*(7060), 862–865. <https://doi.org/10.1038/nature04090>
- [2] Ebbens, S. J. (2016). Active colloids: Progress and challenges towards realising autonomous applications. *Current Opinion in Colloid and Interface Science*, *21*, 14–23. <https://doi.org/10.1016/j.cocis.2015.10.003>
- [3] Martínez-Pedrero, F., Massana-Cid, H., & Tierno, P. (2017). Assembly and Transport of Microscopic Cargos via Reconfigurable Photoactivated Magnetic Microdockers. *Small*, *13*(18), 1–9. <https://doi.org/10.1002/sml.201603449>
- [4] Ebbens, S. J., & Howse, J. R. (2010). In pursuit of propulsion at the nanoscale. *Soft Matter*, *6*(4), 726–738. <https://doi.org/10.1039/b918598d>
- [5] Gijs, M. A. M. (2004). Magnetic bead handling on-chip: New opportunities for analytical applications. *Microfluidics and Nanofluidics*, *1*(1), 22–40. <https://doi.org/10.1007/s10404-004-0010-y>
- [6] Bechinger, C., Di Leonardo, R., Löwen, H., Reichhardt, C., Volpe, G., & Volpe, G. (2016). Active particles in complex and crowded environments. *Reviews of Modern Physics*, *88*(4). <https://doi.org/10.1103/RevModPhys.88.045006>
- [7] Martínez-Pedrero, F., & Tierno, P. (2015). Magnetic Propulsion of Self-Assembled Colloidal Carpets: Efficient Cargo Transport via a Conveyor-Belt Effect. *Physical Review Applied*, *3*(5), 1–6. <https://doi.org/10.1103/PhysRevApplied.3.051003>
- [8] Purcell, E. M. (1977). Life at low Reynolds number. *American Journal of Physics*, *45*(1), 3–11. <https://doi.org/10.1119/1.10903>
- [9] Petukhov, A., Kegel, W., & van Duijneveldt, J. (2011). Colloidal suspensions. *Journal of Physics: Condensed Matter: An Institute of Physics Journal*, *23*(19), 190201. <https://doi.org/10.1088/0953-8984/23/19/190201>
- [10] Tierno, P., Muruganathan, R., & Fischer, T. M. (2007). Viscoelasticity of dynamically self-assembled paramagnetic colloidal clusters. *Physical Review Letters*, *98*(2), 1–4. <https://doi.org/10.1103/PhysRevLett.98.028301>
- [11] Janssen, X. J. A., Schellekens, A. J., van Ommering, K., van IJzendoorn, L. J., & Prins, M. W. J. (2009). Controlled torque on superparamagnetic beads for functional biosensors. *Biosensors and Bioelectronics*, *24*(7), 1937–1941. <https://doi.org/10.1016/j.bios.2008.09.024>
- [12] Osterman, N., Poberaj, I., Dobnikar, J., Frenkel, D., Zihlerl, P., & Babić, D. (2009). Field-Induced self-Assembly of suspended colloidal membranes. *Physical Review Letters*, *103*(22), 2–5. <https://doi.org/10.1103/PhysRevLett.103.228301>
- [13] van Dommelen, R., Fanzio, P., & Sasso, L. (2018). Surface self-assembly of colloidal crystals for micro- and nano-patterning. *Advances in Colloid and Interface Science*, *251*, 97–114. <https://doi.org/10.1016/j.cis.2017.10.007>
- [14] Massana-Cid, H., Meng, F., Matsunaga, D., Golestanian, R., & Tierno, P. (2019). Tunable self-healing of magnetically propelling colloidal carpets. *Nature Communications*, *10*(1), 2444. <https://doi.org/10.1038/s41467-019-10255-4>
- [15] Cao, X., Panizon, E., Vanossi, A., Manini, N., & Bechinger, C. (2019). Orientational and directional locking of colloidal clusters driven across periodic surfaces. *Nature Physics*. <https://doi.org/10.1038/s41567-019-0515-7>